Evaluation of Energy Usage for the First Stage of Heavy Water Production

Rosa-Hilda Chávez
Gerencia de Ciencias Ambientales, Instituto Nacional de Investigaciones Nucleares, Carretera México – Toluca S/N,
La Marquesa, Ocoyoacac 52750, Salazar, Estado de México, México

Javier de J. Guadarrama
Departamento de Ingeniería Eléctrica y Electrónica, Instituto Tecnológico de Toluca, Municipio de Metepec 52140,
Estado de México, México

DOI 10.1002/aic.11327

The thermodynamic analysis of the first stage of enrichment of heavy water production by the Girdler Sulfide (GS) process is described. Use of the Second Law of Thermodynamics as analysis tool allows a simple and useful procedure for the quantification of the transit energy in the process. Such thermodynamic analysis based on the concepts of irreversible entropy increase has frequently been suggested as pointers to sources of inefficiency in chemical processes. Furthermore, this study points out where the irreversibilities of the process are located, a generalized discussion of the cost with respect to the optimization parameters, and provides a generalized discussion from the successful application of the technique. © 2007 American Institute of Chemical Engineers *AIChE J,* 53: 2948–2956, 2007
Keywords: entropy change, heavy water, second law of thermodynamics

Introduction

A Second Law analysis in its simplest form involves a complete evaluation and an account of the energy entering and leaving a process. For more complex processes, this may require systematic decomposition of the overall process into progressively smaller parts until sufficient detail of the energy losses is obtained.[1,2] A Second Law analysis involves the following steps:

1. Obtaining a complete and consistent mass and energy balance.
2. Selecting a reasonable reference atmosphere. Generally, this is atmospheric pressure and adequate values for the temperature of the environmental air, cooling water, or an average of the two.
3. Establishing realistic process boundaries. Selection of the process boundaries defines what feeds, products, and energy usage are to be included in the analysis. Care must be taken in establishing these boundaries so that equipment such as heat exchangers are considered only once in the energy loss calculations.
4. Determining the required thermodynamic properties. Entropy and enthalpy data are required for the calculation of the energy of each stream that crosses the process boundary.
5. Evaluating the minimum energy required for the process. The minimum energy required by the process is defined as the difference between the calculated energy of the product streams and the raw material streams. Whenever the process produces, steam, electricity, or work, these products are included in the minimum energy.
6. Determining actual energy and lost energy. Actual energy is obtained by accounting for the fuel, steam, electricity, heat, and work supplied to the process. The lost energy is simply the difference between the actual energy and the minimum energy.

Correspondence concerning this article should be addressed to R.-H. Chávez at rhch@nuclear.inin.mx

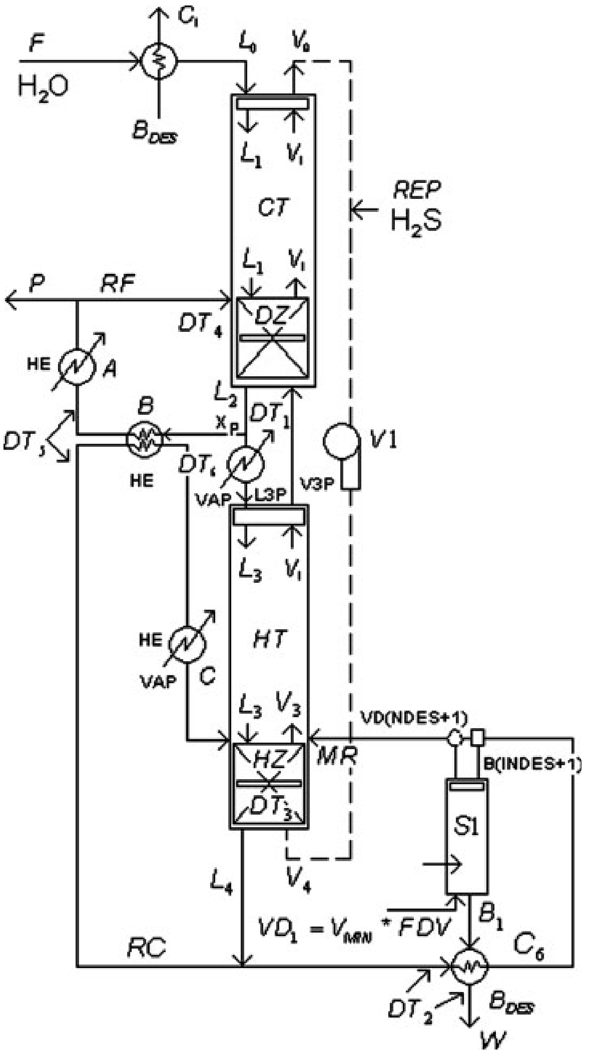

Figure 1. Bi-thermal process flow diagram.

7. Re-analyzing parts of the process having the largest losses in energy. This involves further decomposition of these specific parts of the process and reanalyzing the smaller processing sections to facilitate pinpointing the major contributor to the energetic losses.

First Stage of GS Process

When two streams, natural water and H_2S enriched with deuterium, are in a countercurrent flow at a low temperature (32°C); the latter will exchange its deuterium with the hydrogen of the water until that reaction attains equilibrium. A small part of the enriched water is separated as a product and the rest of the enriched water continues in a countercurrent flow with the impoverished H_2S, but now at a high temperature, where the transfer direction is inverted. It must be remarked that, at a low temperature, the water is enriched in deuterium due to the gas flow, and at high temperature (130°C), the H_2S gets enriched in deuterium due to the water (see Figure 1). The operation lines appear between the two equilibrium lines at the two temperatures mentioned[3] (see Figure 2).

Figures 1 and 2 show that point *F* represents the feeding into the cold tower. The operating line of the cold tower shows the deuterium enrichment in the water up to point *P*, where the final product is obtained. Point *W* is the exit from the hot tower. The arrows on the operating lines indicate the direction of the water flow (see Figure 2). The gas flows in the opposite direction. Undesignated lines are the equilibrium lines. When the operation line appears above the equilibrium line, it indicates that the deuterium transfer is from the gas to the liquid (cold tower, CT, at 32°C). The transfer direction is reversed in the hot tower since in this case the equilibrium line appears above the operating line (hot tower, HT, at 130°C). The slope of the equilibrium line is equivalent to one over alpha, where α is the separation factor. In order to recover the maximum quantity of deuterium in water, it is necessary to maintain a maximum temperature difference between the cold and hot tower, and α maintains the same value even when the temperature increases above 130°C. This is therefore the maximum temperature feasible in the hot tower since α remains invariable at higher temperature. In order to reduce the gas volume needed to operate and increase the H_2S solubility in water, it is necessary to apply constant high pressure of 21×10^5 Pa. This pressure remains constant through the enrichment process.

The feed water L_0 is heated to 32.5°C by the heat exchanger C_1 shown in Figure 1. The deuterium enriched water flows out from under the cold tower; part of it is directed into the hot tower and the other recirculated through the cold tower to cool and dehumidify the hot gas from the hot tower. The recirculated water is cooled by means of the heat exchangers, first B and then A, before being used in the dehumidifying zone.

The deuterium-impoverished water leaves the hot tower and is discarded as a residue. Before leaving the system, the water is mixed with steam in the stripper S_1 to eliminate the H_2S which has dissolved. Together, the H_2S and the steam are introduced into the humidifying zone, and warmed and

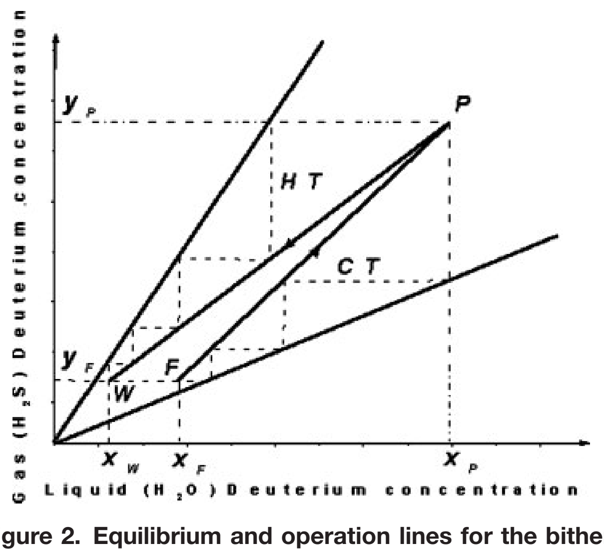

Figure 2. Equilibrium and operation lines for the bithermal process.

humidified by the cold gas from the cold tower. Some of the water which leaves the hot tower is warmed up in heat exchangers B and C, and recirculated throughout the humidifying zone; heat exchanger B transfers heat between the dehumidifying and humidifying recirculation streams. In these conditions, the quantity of cooling water and warming stream is diminished, which results in a lower consumption of energy. The H_2S is circulated within a closed circuit by blower V_1.

The continuous line is water current and the discontinuous line is H_2S flow, CT is cold tower, HT is hot tower, S_1 is the stripper, HE is heat exchanger, V_1 is the blower, DZ is the dehumidifying zone, HZ is the humidifying zone.

A process may be considered as a black box with energy flows coming in and going out at different levels (Figure 3). For example, the process can consume fuel and steam and wasted heat in heat exchangers or refrigerants. In any case, the process will have a finite number of energy sources, and energy drains will handle a finite energy flow.[1,2] The model presented included both temperature and concentrations of multicomponent system in the computation of entropy changes (see Figure 3).

The system is fed by a water stream L_0 at 32.5°C, by a steam to the stripper VD_1 at 216°C and by a restoration stream of H_2S at 32.0°C. The streams which go out from the system are: residual water B_{DES} at 65.3°C and the production stream at 35°C. The system will also exchange heat through the cooling water and the heating steam.

Process Design Model

The process design model in Figure 3 is considered the first stage of heavy water bithermal process flow diagram shown in Figure 1; in this stage the deuterium concentration is below 1000 ppm; the binary mixture is H_2O–H_2S, and the

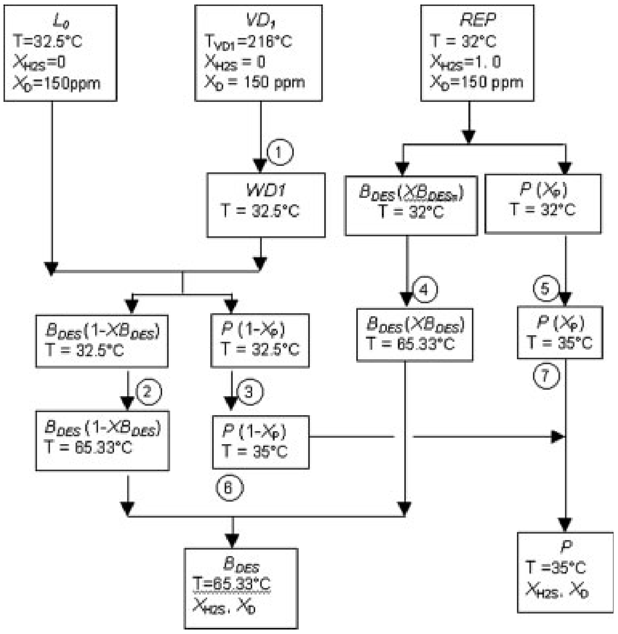

Figure 3. The sequence of the lost work calculation model.

Table 1. Data/Results of the GS Process First Stage

Data	
CT (°C)	32
DL_0 (ppm)	150
DREP (ppm)	150
DVD_1 (ppm)	150
DT_1 (°C)	7.22
DT_2 (°C)	0.03
DT_3 (°C)	27.7
DT_4 (°C)	12.0
DT_5 (°C)	5.55
FVD	3.15
HVD_1 (kJ/kmol)	66,188.285
HT (°C)	130
KTE	1.0
L_0(kmol/h)	87.62
P (kmol/h)	4.54
PRES (Pa)	21×10^5
REL	0.49
T_{ref} (°C)	25
TAE, TAS (°C)	15.5 and 35
$T_{B_{DES}}$ (°C)	216
Results	
Annual equipment cost ($)	282,569.7
Annual energy cost ($)	279649.5
Cost ($)	562,219.2
Cooling water flow (kgmol/h)	635.146
$H_{B_{DES}}$ (kJ/kmol)	4453.6588
Heating steam flow (kmol/h)	3.51
L_1 (kgmol/h)	90.22
L_3 (kgmol/h)	113.31
Q_A (kJ/h)	929,425.392
Q_B (kJ/h)	399,990.4
Q_C (kJ/h)	135,896.32
Q_{C1} (kJ/h)	113,428.24
RC (kmol/h)	94.56
$T_{B_{DES}}$ (°C)	59.8
Transfer $area_A$ (m^2)	12.39
Transfer $area_B$ (m^2)	3.56
Transfer $area_C$ (m^2)	1.41
Transfer $area_{C1}$ (m^2)	0.67
T_{RC} (°C)	59.77
T_{RF} (°C)	16.16
Total transfer area (m^2)	73.96
UA, UB, UC kJ/h m^2 °C)	6084.3728, 6125.376, 7697.7232
V_1 (kgmol/h)	184.128
V_3 (kgmol/h)	211.75
V_{min} (kgmol/h)	2.93
VD_1 (kg/h)	9.25
Vapor flow (kgmol/h)	3.51
W_P (kJ/h)	990,479.5752
ΔS_{gen} (kJ/°C)	3428.5788

Table 2. Simulation Results of 2, 36, and 71 Plates of the Two Deuterium Exchanger Towers*

Parameter	Plate 2	Plate 36	Plate 71
T (°C)	67.22	126.87	32
L (kmol/h)	209.46	91.25	70.012
HL (kJ/kmol)	6352.22	1767.82	1934.59
X_{H_2S}	0.01368	0.01144	0.0
X_P	0.1529×10^{-3}	2.66×10^{-3}	0.15×10^{-3}
V (kmol/h)	142.73	161.48	140.249
HV (kJ/kmol)	2013.50	9458.43	−346.058
y_{H_2S}	0.9832	0.8719	0.9965
y_D	0.7381×10^{-4}	14.97×10^{-4}	0.6806×10^{-4}

*Column 2: Results/plate 2 at the bottom of hot tower. Column 3: results/plate 36 at the stage between hot and cold tower. Column 4: Results/plate 71 at the top of cold tower.

Table 3. Results of Actual Energy Consumed by L_0

L_0 (kmol/h)	72.64	87.622
ΔS_1 (kJ/K)	-1.0293078e^{+02}	-1.2555907e^{+02}
ΔS_2 (kJ/K)	1.0965685e^{+02}	1.3376283e^{+02}
ΔS_3 (kJ/K)	-4.2579133e^{+00}	-4.2579133e^{+00}
ΔS_4 (kJ/K)	2.2114379e^{-03}	2.6975814e^{-03}
ΔS_5 (kJ/K)	-2.0890920e^{-02}	-2.0890920e^{-02}
ΔS_6 (kJ/K)	6.7657479e^{-02}	8.2531159e^{-02}
ΔS_7 (kJ/K)	5.5098520e^{-01}	5.5098520e^{-01}
ΔS_{VD_1} (kJ/K)	7.2648032e^{+02}	8.6222465e^{+02}
ΔS_{CW} (kJ/K)	-1.1443870e^{+02}	-1.4140445e^{+02}
ΔS_{HV} (kJ/K)	2.2660958e^{+02}	2.7642733e^{+02}
ΔS_{gen} (kJ/K)	8.4171921e^{+02}	1.0018087e^{+03}
W_P (kJ)	2.4316334e^{+05}	2.8941142e^{+05}

differences between the properties of HDO and H_2O and between those of HDS and H_2S are negligible.[4] The fundamental equations are:

1. Global mass balance, and also for each individual component
2. Global energy balance, and also for each individual component
3. An equilibrium relationship
4. The component concentrations additions (the molar parts of the mixture) must be equal to 1. Every equation is solved at each equilibrium plate (equilibrium stage), by section (dehumidifying or humidifying zones), and by equipment (two exchange isotopic and stripper towers, six heat exchangers, and one blower).

When the rate and composition of the process streams are known, the isotopic transfer stage number may be evaluated by means of the binary mixture H_2O–H_2S, and the deuterium concentration.

The entropy change due to mass transfer contribution and temperature change will be determined using the "black box" diagram shown in Figure 3. This diagram shows the three feeding streams coming paths into the black box, as well as the two streams leaving paths, with the seven routes between the entering and exiting flows.

The entropy increase of the each stream of the Figure 3 is defined by the following equations, where x_1 are the molar parts of the H_2O and H_2S:

$$\Delta S_1 = \text{VD}_1\left(S_{T=216^\circ\text{C}} - S_{T=32.5^\circ\text{C}}\right) \tag{1}$$

$$\Delta S_2 = B_{\text{DES}}\left(1 - x_{B_{\text{DES}}}\right)Cp_{B_{\text{DES}}} \ln \frac{T_{B_{\text{DES}}}}{T_{\text{ref}}} \tag{2}$$

$$\Delta S_3 = P\left(1 - x_P\right)Cp_P \ln \frac{T_{\text{RF}}}{T_{\text{ref}}} \tag{3}$$

$$\Delta S_4 = B_{\text{DES}}\left(x_{B_{\text{DES}}}\right)Cp_{B_{\text{DES}}} \ln \frac{T_{B_{\text{DES}}}}{T_{\text{REP}}} \tag{4}$$

$$\Delta S_5 = P\left(x_P\right)Cp_P \ln \frac{T_{\text{RF}}}{T_{\text{REP}}} \tag{5}$$

$$\Delta S_6 = -B_{\text{DES}}R\left[x_{B_{\text{DES}}} \ln\left(x_{B_{\text{DES}}}\right) + \left(1 - x_{B_{\text{DES}}}\right) \ln\left(1 - x_{B_{\text{DES}}}\right)\right] \tag{6}$$

$$\Delta S_7 = -P(R)\left[x_P \ln x_P + \left(1 - x_P\right) \ln\left(1 - x_P\right)\right] \tag{7}$$

$$\Delta S_{\text{VD}_1} = 0.000213\text{VD}_1\left(H_{\text{VD}_1} - 504\right) - \Delta S_1 \tag{8}$$

The temperature contribution in the heat exchanger A for cooling water (cw) is:

$$\Delta S_{\text{cw}} = Q_{\text{A}} = \frac{\ln(T_2/T_1)}{T_2 - T_1} \tag{9}$$

The temperature contribution in the heat exchanger C for heating steam (HV) is:

$$\Delta S_{\text{HV}} = \frac{-\sum Q}{T_{\text{vap}}} \tag{10}$$

The total entropy changes are evaluated to determine the actual energy consumed in the process due to all the irreversibilities present in the system. The lost work W_P is evaluated as:

$$W_P = T_{\text{ref}}\Delta S_{\text{gen}} \tag{11}$$

where ΔS_{gen} is the total entropy increase:

$$\begin{aligned}\Delta S_{\text{gen}} = {} & \Delta S_1 + \Delta S_2 + \Delta S_3 + \Delta S_4 + \Delta S_5 + \\ & \Delta S_6 + \Delta S_7 + \Delta S_{\text{VD}_1} + \Delta S_{\text{CW}} + \Delta S_{\text{HV}}\end{aligned} \tag{12}$$

An irreversible process exists when a system is not in equilibrium and undergoes finite changes.

The entropy production is defined as

$$\Delta S = S_{\text{b}} - S_{\text{a}} - \left(\Sigma \frac{Q}{T}\right)_{\text{a}\rightarrow\text{b}} \tag{13}$$

A reversible process leads to attain the minimum consumption of energy. This energy could be in the form of work or of

Table 4. Results of Actual Energy Consumed by FVD

FVD	1.1	1.25	1.6	2	3	3.5
ΔS_1 (kJ/K)	−796.2315	−904.808	−1158.1550	−1447.6937	−2171.5403	−2533.4638
ΔS_2 (kJ/K)	1213.1876	1219.378	1233.8264	1250.3377	1291.6158	1312.2551
ΔS_3 (kJ/K)	−39.2749	−39.2749	−39.2749	−39.2749	−39.2749	−39.2749
ΔS_4 (kJ/K)	0.02446	0.02459	0.02488	0.02521	−0.02604	0.02646
ΔS_5 (kJ/K)	−0.19269	−0.1927	−0.19269	−0.19269	−0.19269	−0.19479
ΔS_6 (kJ/K)	0.74853	0.752352	0.76126	0.77145	0.79692	0.80965
ΔS_7 (kJ/K)	5.08227	5.08228	5.08227	5.08227	5.08227	5.08227
ΔS_{VD_1} (kJ/K)	973.86742	1106.668	1416.53420	1770.66796	2654.32834	3098.66622
ΔS_{CW} (kJ/K)	8388.70662	8217.836	7953.14803	7782.15213	7141.66123	7013.54297
ΔS_{HV} (kJ/K)	−1208.9793	−1279.64	−1304.31262	−1289.194582	−1146.96535	−1125.28136
ΔS_{gen} (kJ/K)	8536.97502	8325.829	8107.4414	8032.68168	7737.21179	7732.16773
W_P (kJ)	4,439,228.18	4,329,432	4,190,765.528	4,176,994.729	4,024,604.244	4,107,757.06

Table 5. Results of Actual Energy Consumed by DT_4

DT_4	10	15	17.5
ΔS_1 (kJ/K)	−2281.15069	−2281.15	−2281.15069
ΔS_2 (kJ/K)	1604.70165	1604.702	1604.700817
ΔS_3 (kJ/K)	−25.2305786	−32.2564	−35.79435849
ΔS_4 (kJ/K)	0.03221154	0.032212	0.032211541
ΔS_5 (kJ/K)	−0.11907668	−0.15485	−0.172866981
ΔS_6 (kJ/K)	0.8283182	0.828318	0.828318195
ΔS_7 (kJ/K)	5.03731843	5.037318	5.037318432
ΔS_{VD_1} (kJ/K)	2790.06567	2790.066	2790.088685
ΔS_{CW} (kJ/K)	7370.23734	7698.163	7702.798392
ΔS_{HV} (kJ/K)	−1292.52128	−1224.03	−1247.578426
ΔS_{gen} (kJ/K)	8171.87918	8561.234	8538.786696
W_P (kJ)	4,249,379.18	4,451,843	4,440,157.032

Table 7. Results of Actual Energy Consumed by ΔH_{VD_1}

ΔH_{VD_1}	20,500	25,500	30,500
ΔS_1 (kJ/K)	−3474.501966	−2616.706235	−2100.250011
ΔS_2 (kJ/K)	1365.918682	1317.001864	1287.550688
ΔS_3 (kJ/K)	−41.4155332	−41.4155332	−41.4155332
ΔS_4 (kJ/K)	0.027546339	0.026559844	0.025965896
ΔS_5 (kJ/K)	−0.203717914	−0.203717914	−0.203717914
ΔS_6 (kJ/K)	0.842766384	0.8125851	0.79441357
ΔS_7 (kJ/K)	5.082279696	5.082279696	5.082279696
ΔS_{VD_1} (kJ/K)	4028.146	3137.925943	2602.280222
ΔS_{CW} (kJ/K)	7128.180384	7210.910616	7395.964752
ΔS_{HV} (kJ/K)	−1000.201936	−1046.620906	−1012.13847
ΔS_{gen} (kJ/K)	8011.85792	7966.812976	8137.687536
W_P (kJ)	4166175.323	4142743.668	4231597.184

heat. Heat and work are seen as different kinds of energies, because heat does not become completely transformed into work, and work does transfer completely into heat. Thus the heat fed to the process is transformed to the mechanical energy equivalent given by the Carnot efficiency. The residual heat will be rejected to the surroundings. The minimum amount of energy necessary to carry out the process is therefore:

$$E_{\min} = W + Q\left(1 - \frac{T_{\text{ref}}}{T}\right)_{\text{rev}} \tag{14}$$

The actual energy is:

$$E_{\text{actual}} = W + Q\left(1 - \frac{T_{\text{ref}}}{T}\right)_{\text{actual}} \tag{15}$$

The difference between actual energy E_{actual} and minimum energy $E_{\min}$ is the lost work W_p due to the irreversibilities of the actual process.

$$W_P = T_0\Delta(S_s M_s) + S_b M_b - S_a M_a - \frac{Q}{T} \tag{16}$$

$$W_P = T_0 \Delta S \tag{17}$$

A steady state process is

$$W_P = T_0\left(S_b M_b - S_a M_a - \frac{Q}{T}\right) \tag{18}$$

The optimization parameters with the greater irreversibilities of the process are: REL, FVD, P, H_{VD1}, L_0, DT_3, DT_4, DT_1. These parameters were chosen to determine the minimum cost for the first stage of heavy water production, since they have direct influence in the dimensioning of the equipments as well as in the energetic consumption. Another important objective was to obtain the values of these optimum parameters according to the investment done in capital costs. This was calculated using the constant KTE with values of 0.5, 1.0, and 2.0, which represent half, total, and twice the investment costs respectively.

Table 6. Results of Actual Energy Consumed by DT_2

DT_2	0.005	0.01
ΔS_1 (kJ/K)	−2366.37249	−2366.47
ΔS_2 (kJ/K)	1346.16518	1346.304
ΔS_3 (kJ/K)	−41.4902343	−41.4902
ΔS_4 (kJ/K)	0.02714866	0.027151
ΔS_5 (kJ/K)	−0.20187013	−0.20187
ΔS_6 (kJ/K)	0.83131687	0.83132
ΔS_7 (kJ/K)	5.03731843	5.037318
ΔS_{VD_1} (kJ/K)	2894.29999	2894.422
ΔS_{CW} (kJ/K)	7263.77964	7263.78
ΔS_{HV} (kJ/K)	−1045.24814	1045.234
ΔS_{gen} (kJ/K)	8056.82755	8057.003
W_P (kJ)	4,189,552.17	4,202,192

Energy Consumption and Equipment Cost Estimation

The determination of the equipment cost and the operation cost sensibility depends completely on the mass and thermal changes of the first section of heavy water enrichment by the GS process.

An optimum economical design is based on the total minimum cost by unit time. The total costs are the addition of annual equipment cost plus annual energy cost.[5] The equations that follow were developed from the graphics presented in Peters et al.[5] and the parameters were obtained from the fitting of the graphics.

What follows is the determination of these costs in the particular units, equipment by equipment and energy consumption, in the first section of heavy water enrichment plant:

1. Isotopic exchange, dehumidifying and humidifying zones and stripper towers

$$\text{Material weight} = \text{Column weight} + \text{Cylinder head weight} \tag{19}$$

$$\text{Tower material cost} = 80.26(\text{Material weight})^{0.7066} \tag{20}$$

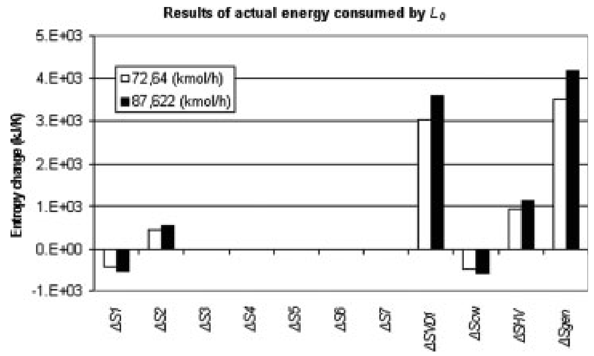

Figure 4. Results of actual energy consumed by L_0.

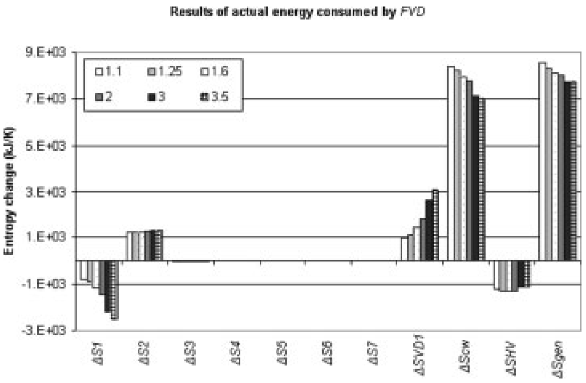

Figure 5. Results of actual energy consumed by FVD.

$$\text{Plate cost} = 270\left(\frac{\text{Plate number}}{\text{Plate efficiency}}\right)(1.2035)^{\text{Diameter}} \tag{21}$$

2. Heat Exchanger

$$\text{Heat exchanger cost} = 846\left(\sum \text{Transfer area}\right)^{0.1565} \tag{22}$$

3. Blower

$$\text{HP}_{\text{Hydraulic}} = 0.148(\text{Molar flow})(\Delta P) \tag{23}$$

$$\text{HP} = \frac{\text{HP}_{\text{Hydraulic}}}{0.7} \tag{24}$$

$$\text{Blower cost} = 195(\text{Volumetric rate})^{0.6092} \tag{25}$$

$$\text{Blower energy} = 18.324\times10^{6}\text{HP} \tag{26}$$

The total equipment cost$^{(\text{TolEquipmCost})}$ is the sum of all the equipment in the process:

$$\text{TotalEquipCost} = \text{Tower material cost} + \text{Plate} + \text{cost} + 6 \times \text{Heat exchanger cost} + \text{Blower cost} \tag{27}$$

And the annual equipment cost is:

$$\text{Anual equipment cost} = \left(\frac{\text{TotalEquipCost}}{\text{Useful service life years}}\right)100 \tag{28}$$

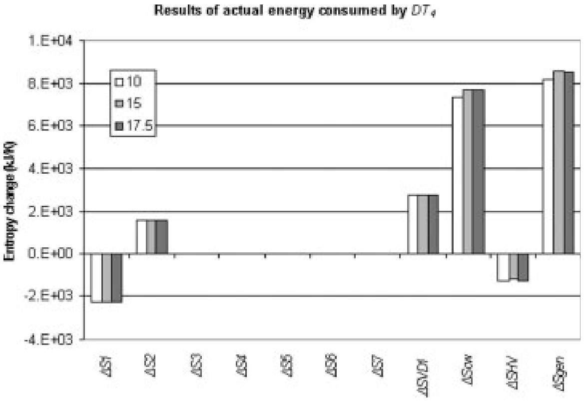

Figure 6. Results of actual energy consumed by DT$_4$.

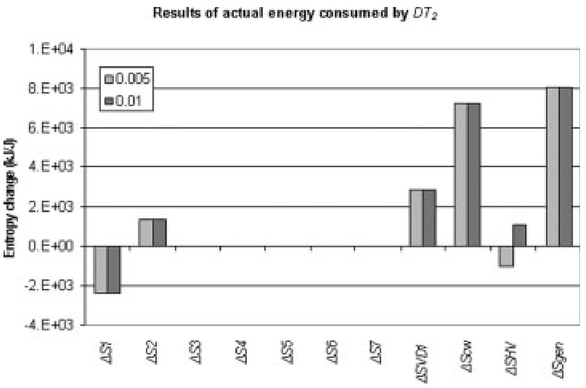

Figure 7. Results of actual energy consumed by DT$_2$.

The total energy cost is the sum of all consumption energy cost of the equipments:

$$\text{Annual energy cost} = (\text{Blower energy} + \text{Lost work} + 6 \times \text{HeatExchLostEnergy})\frac{\text{Cost in \$}}{\text{Energy}} \tag{29}$$

The total cost is the sum of energy annual cost plus fixed annual cost:

$$\text{Total cost} = \text{Annual equipment cost} + \text{Annual energy cost} \tag{30}$$

Results

Table 1 shows data and results of the GS process and Table 2 some of the plentiful simulation results of 2, 36, and 71 plates of the two deuterium exchanger towers. Table 2 (column 2) presents the results of the plate 2 owing at the bottom of the hot tower. Table 2 (column 3) presents the results of the plate 36, and column 4 the results of the plate 71 owing at the top of the cold tower. Other plate values from 3 to 35 and 37 to 70 are not shown due to their abundance. Tables 3–7 show some of the plentiful simulation entropy change results, with the variation of one optimum variable; as L_0 in Table 3, FVD in Table 4, DT$_4$ in Table 5, DT$_2$ in Table 6, $\Delta\text{SH}_{\text{VD1}}$ in Table 7. Tables 3–7 show the entropy changes of each path of the seven routes between the entering and exiting flows of the Figure 3 (ΔS_1, ΔS_2, ΔS_3, ΔS_4, ΔS_5, ΔS_6, ΔS_7) and the temperature contribution in the heat exchanger A (ΔS_{CW}), and C ($\Delta S\text{H}_{\text{VD1}}$),

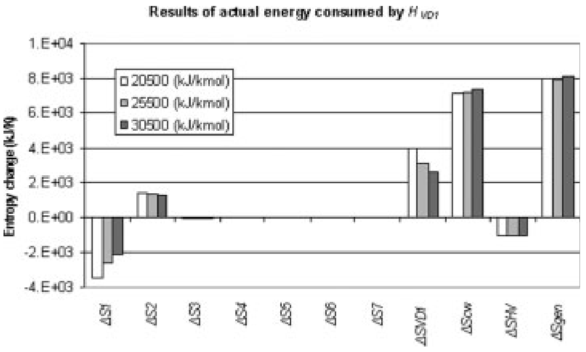

Figure 8. Results of actual energy consumed by H_{VD_1}.

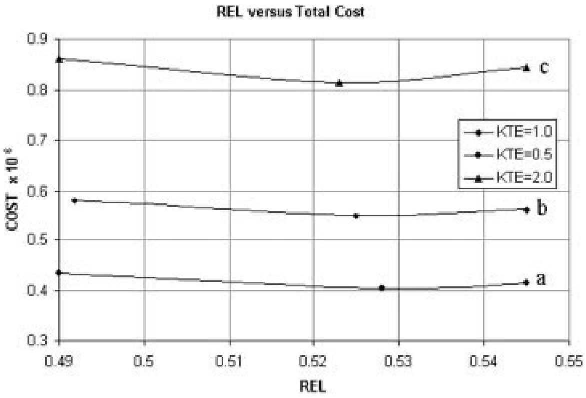

Figure 9. REL = L_1/V_1 vs. total cost.

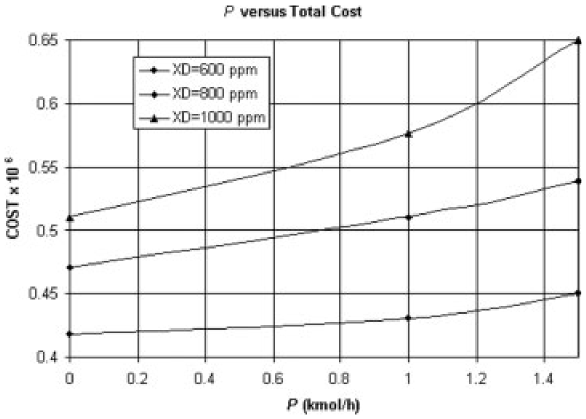

Figure 11. *P* vs. total cost.

the stream feeds in S1 (ΔS_{VD1}), the total entropy changes (ΔS_{gen}) and the lost work of the process (W_P) by temperature and mass transfer changes.

When the gradients for DT_4, FVD, and L_0 increased, they also increased the entropy generation due to temperature changes and to additional quantities processed material required. However, when the parameter H_{VD1} increased, the entropy generation decreased, therefore it could be stated that this parameter is the one that contributed to a larger energy yield in the overall process. This situation depends on the mass of the process for DT_4, FVD, and L_0 and the uses of the energy for H_{VD1}.

Table 3 shows ΔS_{VD1} is the biggest entropy change with the variation of L_0, with 726.4803 kJ/K at 72 kmol/h and 862.2246 kJ/K at 87.633 kmol/h, followed by ΔS_{HV} and then ΔS_2 as irreversibilities of the process. Table 4 shows ΔS_{CW} is the biggest entropy change with the variation of FVD, with 8388.7066 kJ/K at 1.1 and 8217.836 kJ/K at 1.25, followed by ΔSH_{VD1} and then ΔS_2 as irreversibilities of the process. Table 5 shows ΔS_{CW} is the biggest entropy change with the variation of DT_4, with 7370.2373 kJ/K at 10. and 7702.7983 kJ/K at 17.5, followed by ΔSH_{VD1} and then ΔS_2 as irreversibilities of the process. Table 6 shows ΔS_{CW} is the biggest entropy change with the variation of DT_2, with 7263.7796 kJ/K at 0.005 and 7263.78 kJ/K at 0.01, followed by ΔSH_{VD1} and then ΔS_2 as irreversibilities of the process. Table 7 shows ΔS_{CW} is the biggest entropy change with the variation of ΔH_{VD1}, with 7128.1803 kJ/K at 20555 kJ/K and 7395.9647 kJ/K at 30500 kJ/K, followed by ΔSH_{VD1} and then ΔS_2 as irreversibilities of the process. All negatives entropy exchanges reduce the entropy changes of the process. Figures 4 to 8 show entropy change values of the seven routes between the entering and exiting flows described in Figure 3. Figure 4 describes L_0 variation at 72.64 and 87.622 kmol/h; Figure 5 shows FVD variations at 1.1, 1.25, 1.8, 2, 3, and 3.5; Figure 6 DT_4 variations at 10, 15 and 17.5°C; Figure 7 DT_2 variations at 0.005 and 0.01°C; and Figure 8 H_{VD_1} variations at 20500, 25500 and 30500 kJ/kmol.

1. REL = L_1/V_1 vs. costs

Figure 9 shows the ratio of liquid flow and gas flow in the cold tower, that is to say, the operation line slope, compared to the total cost of the process. Curve b is equivalent to twice the energy cost of curve a, and. Curve c is equivalent to twice the equipment cost of curve b. It is observed that the minimum value of the three curves lies between 0.52 and 0.53. It is concluded that if the equipment or operation costs increase, the optimum value of the operation line slope in the cold tower will not vary significantly with respect to the total minimum cost.

2. FVD vs. costs

FVD is the factor which multiplies the minimum flow of the saturated vapor and feeds the stripper to recover the H_2S of the remainder stream. The minimum cost of the FVD factor is

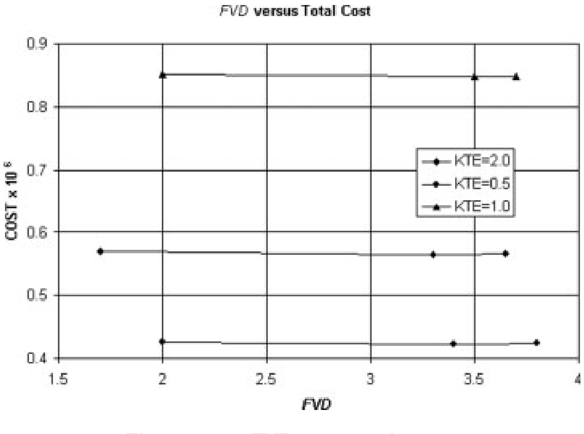

Figure 10. FVD vs. total cost.

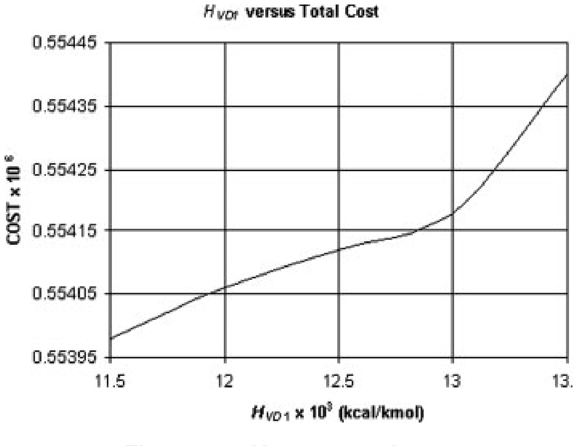

Figure 12. H_{VD_1} vs. total cost.

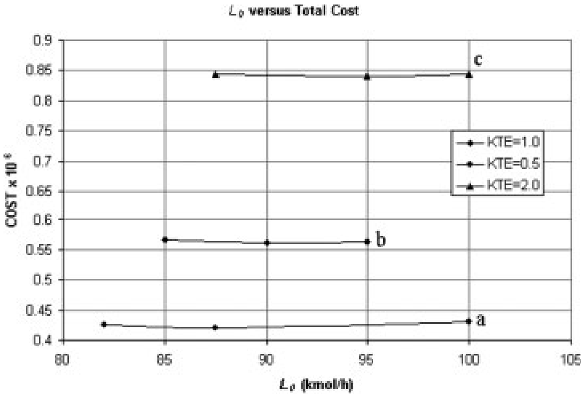

Figure 13. L_0 vs. total cost.

within a 3.15 value. This parameter does not differ significantly from that of the minimum cost in the case of three curves when the equipment or operation costs increase (see Figure 10).

3. *P* vs. costs

   Figure 11 compares total production cost against product flow which satisfies final enrichment of the production. Each curve shows a growing tendency of production cost as production rate increases; however, as the enrichment grade increases, the asymptotic behaviour rises more rapidly with respect to the ordinate axis.

4. H_{VD1} vs. costs

   Figure 12 shows the enthalpy behavior of the vapor feeding to the stripper against the total production cost. If the saturated vapor is sufficient to eliminate H_2S from the residual stream, it becomes economically unfeasible to have a vapor of a higher caloric potential.

5. L_0 vs. costs

   In Figure 13 are presented the curves that show the feed stream to be processed vs. the total cost of production. The minimum cost of curve a is within L_0 = 86.26 kgmol/h; the minimum cost of curve b is within L_0 = 90.8 kgmol/h, and the minimum cost of curve c is within L_0 = 94.43 kgmol/h. In this case L_0 depends upon whether the equipment or the operating cost has been increased.

6. DT_3 vs. costs

   Figure 14 shows the temperature difference between the liquid and the vapor streams in the first stage of enrichment of the humidifying zone hot tower against total production cost. A slight change in the DT_3 parameter can be seen in the three cases.

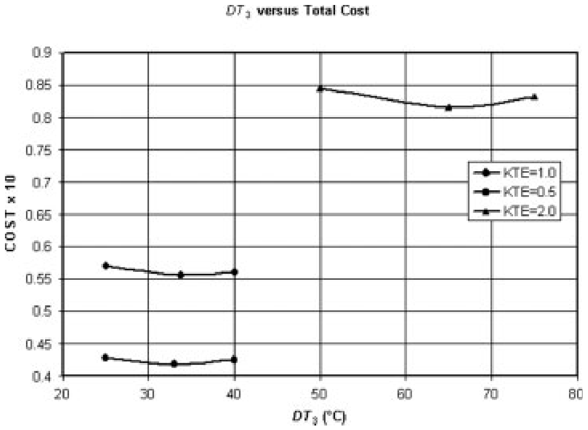

Figure 14. DT_3 vs. total cost.

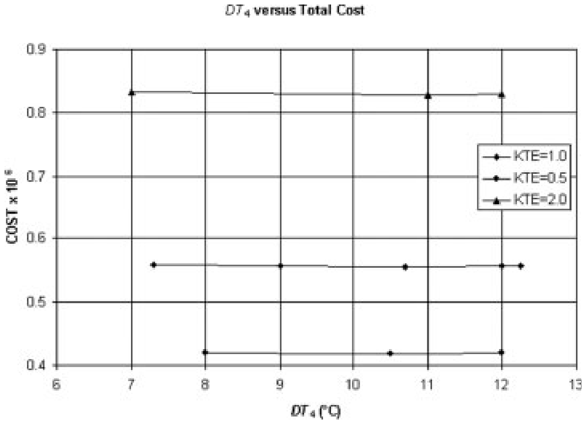

Figure 15. DT_4 vs. total cost.

7. DT_4 vs. costs

   Figure 15 shows the temperature differences between the maximum temperature and the actual temperature of the recirculation stream in the cold tower. A slight change in the DT_4 parameter can be seen in the three cases shown.

8. DT_1 vs. costs

   Figure 16 shows the temperature difference between the gas and the liquid streams in the lower part of the dehumidifying zone DT_1 parameters in the three cases. It is concluded that if the equipment or operation costs increase, the optimum value of the operation line slope in the lower part of the dehumidifying zone will not vary significantly with respect to the total minimum cost.

9. In inflationary processes in which the costs of equipment and energy undergo nonparallel increases, it was determined that the temperature gradients were not altered from their optimal values. Parameters such as the feed stream, slope of the operation line at cold tower (L_1/V_1) and the factor (REL) that multiplies to the minimum steam of the stripper (FVD), showed a smooth dependency to the fluctuations of the equipment and energy costs.

10. It can be seen in Figures 11 and 13 the influence of the costs based on the production capacity and the size of the industrial plant. These figures indicate that L_0 presents a minimum cost to a given production and degree of enrichment; whereas for a constant feed stream, the expenses of

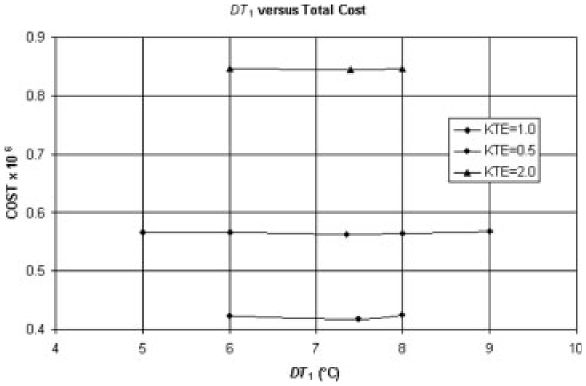

Figure 16. DT_1 vs. total cost.

production and degree of enrichment increase quickly and with asymptotic behavior.

Conclusions

1. The simple equations obtained to evaluate entropy calculations can also be considered in process design calculations. These equations prove useful in determining the temperature and mass transfer changes through all the process.
2. The fact that the parameters: (i) the feed rate L_0, (ii). The cold tower operation line slope L_0/V_1, and (iii) the FVD factor and H_{VD1}, depended on the bulk of the equipments and the energy requirements of the plant.
3. The optimum gradients were obtained based on the irreversible processes. In this evaluation it was found that the major irreversibilities in the deuterium enrichment plant were found in the temperature exchange, such as the flows in the humidifying zone and in the recirculation stream in cold tower.
4. Mass transfer changes were insignificant because the deuterium enrichment was very low from 145 to 600 ppm, as can be seen for the values of ΔS_4, ΔS_5, ΔS_6, and ΔS_7. This behavior was also found in ΔS_3, where the temperature change was very low, from 32.5°C to 35°C).
5. When the gradients for DT_1, DT_3 and DT_4, and L_0 and P increased, they also increased the entropy generation due to temperature changes and to additional quantities processed material required. However, when the parameters, REL, FVD, and H_{VD1} increased, the entropy generation decreased, therefore it could be stated that these parameters are the ones that contributed to a larger energy yield in the overall process.
6. When the gradients for DT_4, FVD, and L_0 increased, they also increased the entropy generation due to temperature changes and to additional quantities processed material required. However, when the parameter H_{VD1} increased, the entropy generation decreased, therefore it could be stated that this parameter is the one that contributed to a larger energy yield in the overall process. This situation depends on the mass of the process for DT_4, FVD, and L_0 and the uses of the energy for H_{VD1}.
7. The results of the optimization can be used in basic engineering for the design and operation of deuterium enrichment plants by GS process.

Acknowledgments

The authors acknowledge the contribution of Mr. Cesar Garcia-Atanacio in preparing the figures. Partial financial support was provided by Consejo Nacional de Ciencia y Tecnología (CONACYT) project I36297-U, and Secretaría de Relaciones Exteriores.

Notation

Process data

B_{DES} = leaving stream from stripper, kmol/h
C_p = heat capacity at constant pressure, kJ/kmol °C
E_{min}, E_{actual} = the minimum and actual amount of energy to carry out the process, kJ/h
F = water feed flow, kmol/h
HL = liquid enthalpy on each plate, kJ/kmol
HV = gas enthalpy on each plate, kJ/kmol
L = liquid flow on each plate, kmol/h
M_{CW} = cooling water mass flow, kmol/h
M_{hv} = heating vapour in the heat exchanger, kmol/h
N_{irrev} = the efficiency of an irreversible thermal engine
P = enriched water flow, kmol/h
Q = heat transfer in heat exchanger, kJ/h
Q_{rev}, Q_{irrev} = thermal energy on reversible and irreversible cycle process, kJ/h
REP = water-impoverished flow
R = ideal gas constant, kJ/kmol K
RF = recirculated flow at cold tower, kmol/h
RC = recirculated flow at hot tower, kmol/h
S, ΔS = entropy and entropy change, kmol/(h °C)
T = temperature of each plate, °C
T_0 = temperature at L_0line, °C
$T_{L_{DES}}$ = temperaure at B_{DES} line, °C
T_{REP} = temperature at H_2S replacement, °C
T_{RF} = temperature at RF stream, °C
T_{vap} = stream temperature, °C
V = gas flow on each plate, kmol/h
VD_1 = feed saturated stream at stripper, kmol/h
V_{MIN} = minimum feed saturated stream at stripper, kmol/h
W = impoverished water flow, kmol/h
W_P = lost work, kJ/h
X = H_2S molar fraction on liquid flow plate
$X_{B_{DES}}$ = H_2S concentration at stripper exiting flow, ppm
X_D = Deuterium molar fraction on liquid flow plate
X_P = H_2S concentration at product flow, ppm
y = H_2S molar fraction on gas flow plate
y_D = Deuterium molar fraction on gas flow plate
α = the separation factor
λ = latent heat, kJ/kg h
ΔP = pressure drop in blower, mmWG/m
Subscripts 1, 2 = initial and final state, respectively

Driving forces parameters

DT_1 = temperature difference between liquid and gas stream at the bottom in the cold tower, °C
DT_2 = temperature difference between the residue stream and liquid leaving stream from humidity zone in hot tower, °C
DT_3 = temperature difference between liquid and gas stream at the bottom in the hot tower, °C
DT_4 = temperature difference between the maximum temperature and actual temperature of recirculation stream in cold tower, °C
DT_5 = temperature difference between cold and hot recirculation stream in dehumidity and humidity zones, °C
H_{VD1} = enthalpy of vapour inside the stripper, kJ/kmol
FVD = A factor, which multiplies the minimum flow of saturated vapour and feeds stripper to recover H_2S from residue
L_0 = feeded water flow, kmol/h

Literature Cited

1. Linnhoff B, Eastwood AR. Overall site optimization by pinch technology. *Trans Inst Chem Eng Part A: Chem Eng Res Des*. 1997;75: S138–S144.
2. Bejan A. *Advanced Engineering Thermodynamics*. New York: John Wiley, 1988.
3. Lena O, Wilhelmsen K. Production of heavy water, an analysis from export control point of view. Stockholm: Swedish Nuclear Power Inspectorate. 38 p. Available from INIS in electronic form, 2003.
4. Chávez RH. Study of the first section of an enrichment plant for heavy water by the girdler sulfide process. MS Thesis, Mexican National Polytechnic Institute (IPN), Mexico DF, 1985.
5. Peters MS, Timmerhaus KD, West RE. *Plant Design and Economics for Chemical Engineers*, *5th ed.* Kogakusha: McGraw Hill, 2003.

Manuscript received Jan. 8, 2007, and revision received Aug. 23, 2007.